SMAR 2019 – Fifth Conference on Smart Monitoring,
Assessment and Rehabilitation of Civil Structures

SMAR 2019

Towards predictor development for assessing structural integrity of components made from wood materials using Acoustic Emission monitoring and signal analysis

Franziska BAENSCH [1], Andreas J. BRUNNER [2]

[1] Bundesanstalt für Materialforschung und -prüfung, Berlin, Germany

[2] Empa, Eidgenössische Materialprüfungs- und Forschungsanstalt, Dübendorf, Switzerland

Contact e-mail: franziska.baensch@bam.de

ABSTRACT: Against the background of sustainable resource management and efficiency, wood-based materials are currently experiencing a revival and, among others, plywood, Laminated Veneer Lumber and glued laminated timber are becoming increasingly more important in the building sector. Even though these materials are so-called engineered products, the element wood is naturally grown with intrinsic variability in mechanical properties and requires professional handling on-site. Otherwise, load-bearing structures made of wood materials may entail certain risks. Critical situations can, in principle, be avoided by implementing a structural health monitoring system into components or structures made from wood material. The aim is to indicate accumulation of mechanical damage and to eliminate or at least significantly reduce the risk of unexpected failure. Toward this purpose, the failure behavior of several layered wood materials under quasi-static tension was investigated in laboratory-scale experiments by means of acoustic emission (AE) measurement. Based on spectral analysis and pattern recognition, two classes of AE signals are identified for each investigated lay-up that are characterized by either low or high frequency contents in the respective power spectra. AE activity and intensity of both signal classes are analyzed, striving for predictors appropriate for AE monitoring concepts.

1 INTRODUCTION

Long-term use of structures or their load-bearing elements made from any material requires maintenance and hence periodic assessment of structural integrity for ensuring safe use, especially in view of changing service loads. These can be induced by more severe environmental factors (e.g., increasing exposure to wind and precipitation due to climate change) or to higher frequency of use or higher service loads (e.g., higher speeds of traffic on transportation infrastructure and resulting dynamic loads). One approach for ensuring structural integrity is implementation or integration of a system for permanent condition monitoring or periodic integrity checks. Acoustic Emission (AE) monitoring has advantages in terms of applicability under service conditions, sensitivity to microscopic damage mechanisms, as well as coverage of the full volume of structures with limited intrusion. However, most criteria for evaluating structural integrity, remaining service life-time, or the extent of required maintenance and repair based on AE are essentially empirical and typically require a data base comprising a large number of tests for sufficiently accurate evaluation and prediction. Examples are procedures using Felicity-ratio from step-wise load tests, or combinations with that and indications from AE activity and AE intensity analysis in a severity measure or a historic-index (Fowler et al. 1989, Chen et al. 2007).

Recent progress in location and identification of the microscopic source mechanisms of the AE signals, e.g., using pattern recognition combined with multi-physics simulations or with nondestructive test data (e.g., X-ray computed tomography), in principle, yields detailed damage maps of located damage events and their type. However, as discussed by Brunner (2018), such damage maps require suitable damage models for quantitative evaluation of structural integrity or for service-life estimates. The question of how AE signal pattern recognition from selected load tests on laboratory-scale and miniature specimens made from solid wood, wood materials, and adhesively bonded wood joints can be used for establishing a predictor for assessing structural integrity or service life of wood structures or load-bearing components is discussed.

2 MATERIALS AND TEST METHODS

The discussed examples are several types of layered wood materials (Fig. 1, left and center) subjected to quasi-static tensile loads to failure monitored by acoustic emission (AE) under laboratory conditions. A “model” cross-ply wood material (CP) was manufactured from three plates of clear spruce wood (without pre-damages and visible defects) that were planed down to 3 mm thickness. Plywood 4 (P4) and 6 (P6) with 4 and 6 veneer layers, respectively, were industrially produced and contain pre-damages introduced into the veneers while rotary peeling the veneers from the trunk. The middle layer of P4 consisted of two cross oriented veneers which, under tension load, showed significant fracture patterns of rolling shear. The core of P6 was made of two unidirectional oriented veneers reinforcing the material in direction of tensile load application. Hence, P6 showed a distinct plastic deformation at large stress. Aforementioned materials were tested based on DIN 52377 (2016) with a specimen size of 400 mm length, 50 mm width and 20 mm thickness. For comparison purpose, solid wood samples made of clear spruce wood were tested, too.

In order to investigate the underlying microscopic damage mechanisms, miniature specimens of 30 mm length were manufactured from wood lamellas of approximately 2 mm thickness with different lay-ups (Fig. 1, right). To focus on the different damage mechanisms in unidirectional and cross directional loaded wood as well as on the role of the adhesive in the layered structure, several orientations of cell arrangement and adhesively bonded lay-ups were subjected to tensile load and monitored by means of AE measurement and, simultaneously, by synchrotron radiation micro computed tomography (SRμCT) imaging (Ritschel et al. 2014, Baensch et al. 2015).

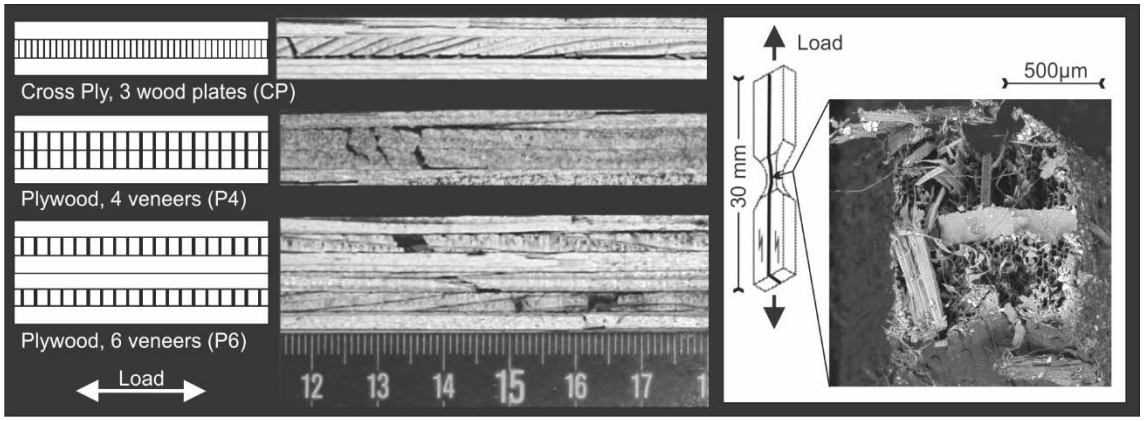

Figure 1. Layered wood materials tested under quasi-static tension load and typical fracture patterns. Left: Cross section of the materials tested based on DIN 52377. Center: Fracture patterns after ultimate tensile failure. Right: ESEM picture of the fracture pattern from a tensile loaded miniature specimen made of two unidirectional oriented wood layers that were adhesively bonded.

3 IDENTIFICATION OF AE SOURCE MECHANISM

AE signals from damage accumulation and crack growth carry information on the source mechanisms, but the assignment of the mechanism to a specific signal is one of the biggest challenges in AE monitoring. Besides conventional parameter analysis of the AE time signals, rather the frequency spectrum of these signals provides indicators of the source's nature. Mathematical approaches like neuronal networks or unsupervised pattern recognition, respectively, based on features of the AE frequency spectrum, enable the identification of natural classes of AE signals.

For the discussed examples, signal classification was performed by means of the unsupervised pattern recognition approach published by Sause et al. (2012). For all specimens discussed here, two classes of AE signals were obtained, independent of the lay-up or specimen size. The signals in both classes essentially differ with respect to higher shares of low and high frequency components (Fig. 2). The average low and high frequency components for the two clusters are influenced mostly by the specimen size, since the miniature specimens yield somewhat higher weighted peak frequencies (Sause et al. 2012) for the respective classes than the standard-size specimens. The different mesoscopic and macroscopic failure behavior of the tested materials, however, is not reflected in the identified AE signal classes (Ritschel et al. 2014). Hence, it is assumed that fundamental phenomena of damage are described by these two classes.

By implementation of model AE signal sources into a finite element model, it was shown that the source excitation time, and thus the crack opening speed, has the strongest impact on the AE frequency spectrum. It is hence assumed, that the low frequency class (c1) was generated by (slower) cell separation and shear processes, while the AE class (c2) with higher frequency components is related to (faster) cell wall cracks and fibre breaks (Vergeynst et al. 2014).

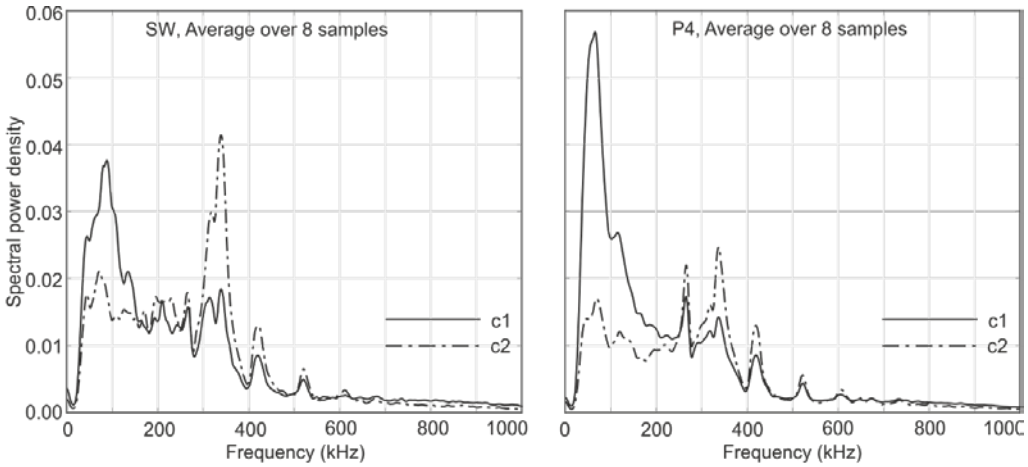

Figure 2. Frequency spectra of two AE signal classes c1 and c2 identified by unsupervised pattern recognition for tension tested solid spruce wood (SW) and plywood (P4) specimens.

4 DISCUSSION ON AE PREDICTORS FOR MONITORING CONCEPTS

4.1 AE activity and material strength

Typically, cumulative AE activity represented by the number of AE signals (called "hits") or AE counts (number of signal acquisition threshold crossings per hit) as a function of time or load shows a steady increase up to failure in quasi-static load tests. The curves (one example for P4 shown in Fig. 3a) are either approximated by two linear curves, one at low, the other at high times

and loads, respectively, or as an exponential curve. If this bilinear representation is chosen, the intersection of the two linear curves yields the so-called "knee"-point (Jinen 1991, Ichikawa et al. 2014). If the curve is interpreted as an exponential curve, which can be validated by overlaying the cumulative curve and the rate curve (the latter suitably scaled), the exponential factor "α" in the exponential $e^{\alpha t}$ describing the AE activity increase with time indicates whether the damage accumulation is faster or slower (Brunner et al. 1995, Brunner et al. 2006). It could be hypothesized that a low value of "α" correlates with a higher failure strength and a high value of "α" with a lower. It is not clear at present whether this can be really quantified and used for prediction of failure and which level of load (in percent of failure load) would have to be achieved for this. If, on the other hand, two linear curves are used to approximate the AE activity behavior as a function of strain, the knee-point could be interpreted as a transition from distributed microscopic damage to coalescence of defects to mesoscopic or macroscopic damage at the location of ultimate failure. For the plywood specimens, the damage accumulation within the initial state of the AE activity curves below the knee-point is found to correlate with its ultimate strength (Fig. 3b). At approximately 70% of ultimate tensile strength (UTS) the state of accelerated damage accumulation (2nd rate, knee-point) sets in, whereby the reinforcing, fibre breaks within the unidirectional oriented layers play an important role.

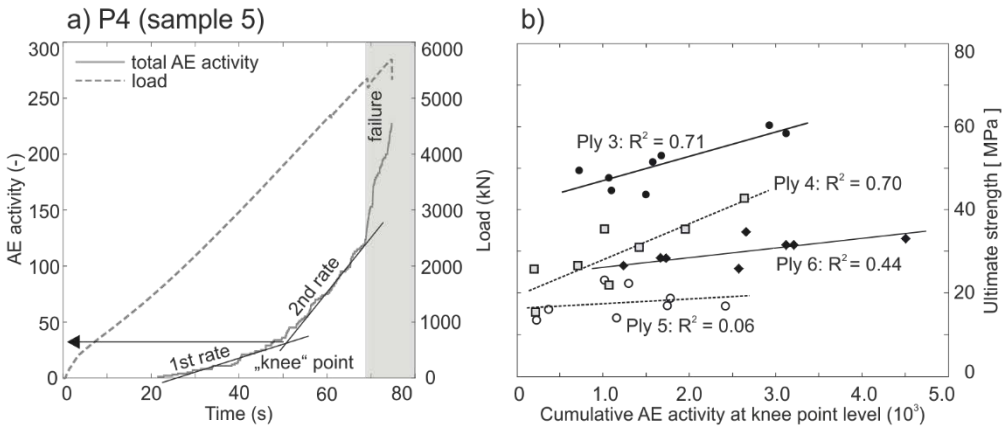

Figure 3. a) Principle of the bi-linear approach in cumulative AE activity shown at plywood P4 sample 5 (compare Figure 4b). b) Correlation between ultimate tensile strength of plywood materials and their cumulative number of AE activity due to development of initial damages.

Table 1. Percent ratio of low frequency class 1 (c1) signals compared to the total AE

Class 1	Ratio of Class c1 signals	Ratio of energy up to 0.85 UTS	Ratio of energy up to UTS
	(%)	(%)	(%)
SW	70 ± 20	73 ± 38	40 ± 48
CP	94 ± 4	90 ± 14	94 ± 6
P4	82 ± 8	77 ± 38	86 ± 29
P6	85 ± 12	89 ± 21	81 ± 31

UTS…ultimate tensile strength

Furthermore, for glass-fiber-reinforced polymer (GFRP) composites it was shown that the AE hit rate in "hits per second" may indicate different damage mechanisms dominating the failure behavior with progressing stress (Brunner et al. 1995, Warnet et al. 2003). However, for the layered wood materials, significant increases in hit rate occur very suddenly and very shortly before ultimate failure (Fig. 4, upper graphs), and thus, the hit rate is rather unsuitable as predictor.

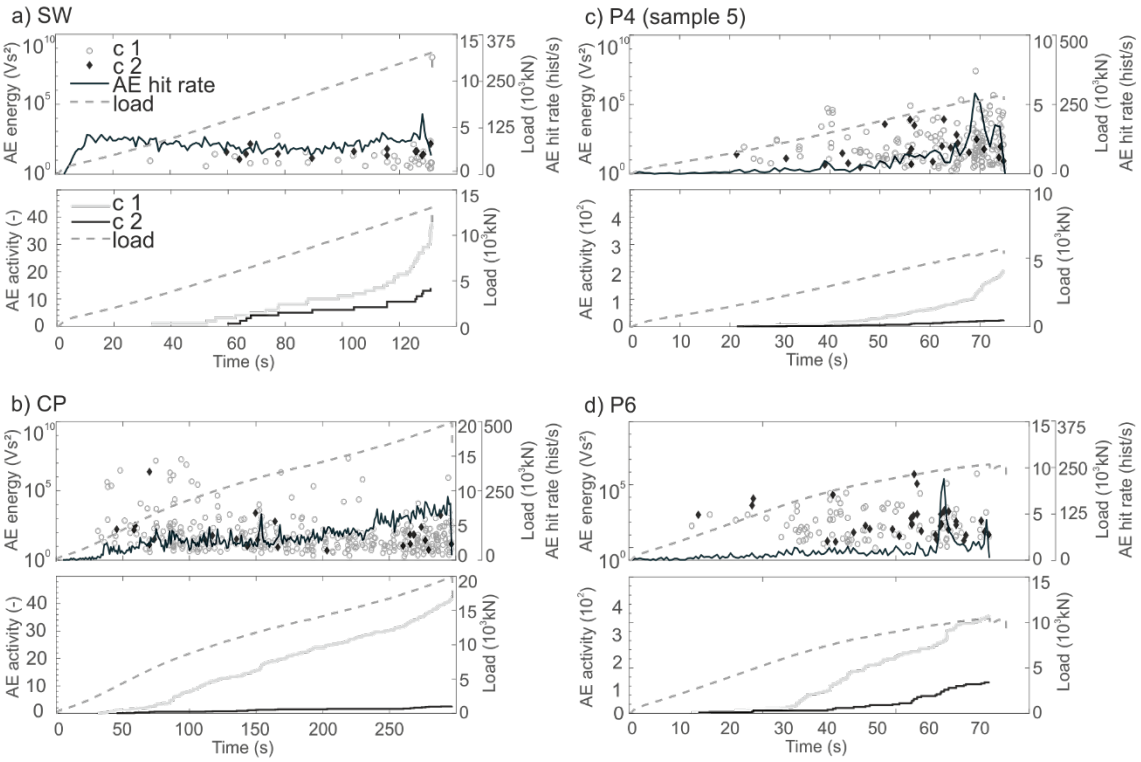

Figure 4. AE signal rate (in hits per second) of the total detected AE during test, AE activity and AE energy plots differentiating the AE classes C1 and C2 for a) the solid spruce wood (SW), for b) the manufactured cross ply CP and plywood c) P4 and d) P6.

4.2 AE signal classes under progressive stress

To possibly identify SDDM during load history of the layered wood materials, the occurrence and intensity of the determined AE signal classes c1 and c2 was analyzed (Fig. 4). For all materials, roughly 70% of the detected AE events are identified as AE signals of class c1 (Table 1). Thus, the activity curve of total AE (Fig. 3a) is clearly ruled by the occurrence of the c1 signals. Further, the appearance of c1 or c2 signals during load history seems to be randomly and cannot be correlated with any state of damage accumulation and failure development.

Distinguishing the AE intensities of single signals of the classes c1 and c2, signals of both classes can achieve approximate AE energy values (Fig. 4). Hence, in terms of cumulative AE energy, e.g., in ratio of energy up to 0.85 UTS level or close to ultimate failure, the clear dominance of c1 is diminished as revealed in the high dispersion (Table 1) for SW, P4 and P6. Especially in case of SW the c1 might rule the failure by a chance of fifty-to-fifty. The CP, manufactured from clear wood plates, represents an exception since c1 was identified to dominate the damage evaluation with high shares in events as well as in AE energy. This is consistent since CP undergoes less rolling shear compared to P4, thus, as soon as the damage accumulation drifts into the outer, unidirectional layers, both layers would fail in a very brittle manner close to each other

resulting in ultimate failure. Since the events of the ultimate failure are excluded for the AE analysis, fibre breaks and the assigned AE signals of class c2 are mostly excluded, too. In case of P4, one of the outer, unidirectional oriented layers can fail clearly earlier than the other due to the distinct shear between both layers.

The AE energy is mainly characterized by the peak amplitude of the signals and its duration. Figure 5 reveals c1 and c2 with the same range in peak amplitudes, but c1 signals are also undergoing longer durations as it is the case for the c2 signals. Gostautas (2007) located different damage mechanisms within a Duration vs. Amplitude graph for GFRP materials to emphasize relevant parameters for predictive monitoring. Comparing his results (see Fig. 3.7 in the report by Gostautas 2007), the signals c1 might be assumed to contain mechanical rubbing or friction, delamination as well as matrix cracking, whereas the source of c2 signals as crack growth. The duration-amplitude range (area) identified as "GFRP delamination" by Gostautas (2007) comprises relatively low amplitudes (45-55 dB) and high durations (1000-10000 µs). Interpreting a delamination in FRP as the result of a large number of matrix microcracks (as discussed by Brunner 2018) the classes c1 and c2 observed in wood materials could also be interpreted as cracks, simply differing in their size. Gostautas (2007) also noted that the position of the signals in the plot may be affected by signal attenuation effects from propagation in the material (which would reduce the amplitude, and possibly also the duration, i.e., shifting them to the left and possibly also downward), and that some of the areas assigned to different mechanisms do overlap to some extent. Hence, the source identification based on this plot might be questionable and delamination processes could be described as larger scale cracks. The crack growth often is the consequence of fibre breaks which always occur in combination with matrix and shear cracks. For layered wood structures under tension, the material strength becomes minimized as soon as fibres break within the reinforcing unidirectionally oriented layers. Furthermore, the energy c2 signals reach increasing energy contents with progressive time and load level (Fig. 4 b, d). Crack growth assigned to c2 signals is of high relevance for load bearing wooden structures.

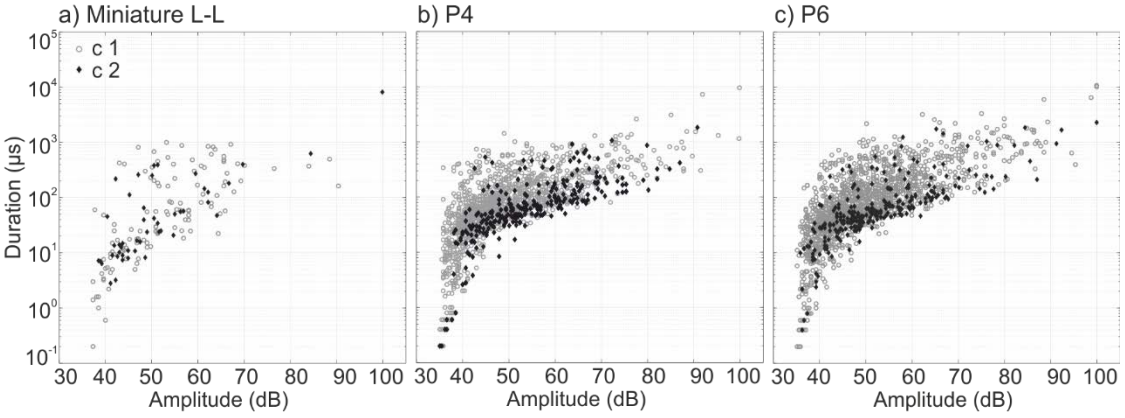

Figure 5. The distribution of AE signals of classes c1 and c2 plotted as Duration vs. Peak Amplitude of the signals is presented for a) a miniature specimen L-L of two longitudinal oriented wood layers made of clear spruce wood bonded together and for standard-size specimens of the plywood materials b) P4 and c) P6.

4.3 Amplitude distribution of AE classes under progressive stress

Features of AE energy of the signal class c2 might provide evidence for failure relevant damage accumulation, and hence, might turn out energy-based parameters for failure predictors for wood materials. As the signal peak amplitude is found to correlate with the magnitude of the crack (Lysak 1996), the evaluation of the slope of the amplitude distribution, the so-called b-value,

might provide insight for differentiating between c1 and c2 (Fig. 6). For monitoring predictor, the amplitude distribution needs to be evaluated at several load stages to proof possible changes of the b-value (slope) of relevance. Herein, the amplitude distribution has been determined before knee-point at 65% and after the knee-point in AE activity at 85% and 95% of the UTS.
For SW, amplitude distribution reveals that c2 signals with peak amplitudes above 60 dB did not occur below 85% of UTS. A decreasing slope in the distribution of c2 signals at peak amplitudes larger than 55 dB might signalize the imminent failure. In the case of P4, whose damage evaluation is governed by strong shear behavior at lower load levels, for peak amplitudes between 45 dB and 60 dB, at 65% of UTS the c1 and c2 signals show more or less the same slope in amplitude distribution, but at 85% of UTS, compared to the c1 signals, the slope flattens for the c2 signals measurable in b-values becoming smaller with progressive stress. In contrast, for P6, which forms fibre breaks and crack growth already at early load stages, the differentiation between amplitude distribution of c1 and c2 is not clear and hence not considered to be meaningful.

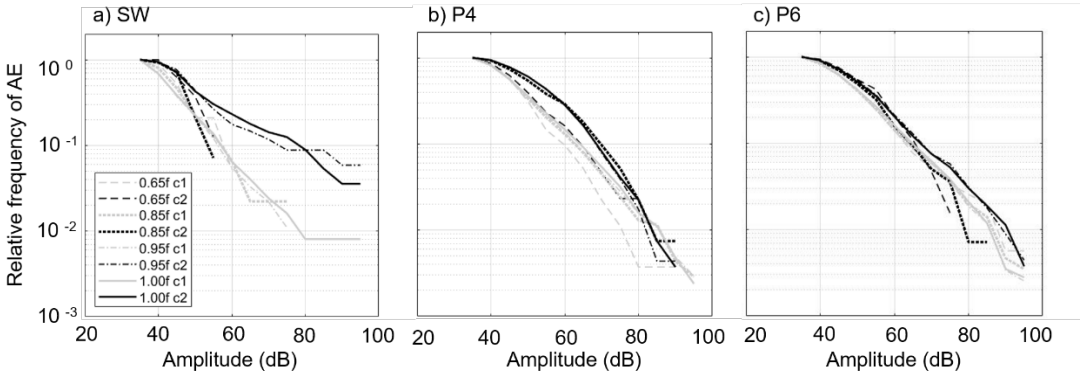

Figure 6. Peak amplitude distribution at 65%, 85% and 95% of ultimate tensile strength as well as for the detected AE until ultimate failure of a) the solid wood (SW) and of the plywood materials b) P4 and c) P6.

5 CONCLUSION BASED OF RESULTS ON PLYWOOD MATERIALS

- The total AE hit rate only increases significantly shortly before failure and hence is unsuitable for quantitative predictions.
- Describing the total AE activity curve by the bilinear approach indicated the onset of the 2nd rate of located AE events at approximately 70% of ultimate tensile strength.
- Independent of plywood material and sample size, two signal classes were identified by means of unsupervised pattern recognition differing with respect to higher shares of low and high frequency components. The low frequency class (c1) is assigned to (slower) cell separation and shear processes, while the class (c2) with higher frequency components is related to (faster) cell wall cracks and fibre breaks.
- Signal class c1 and c2 occurred randomly in time and load history and achieved comparable ranges in AE signal energy.
- A separation of predictive parameters based on the Duration vs. Peak amplitude graphs failed. The multi-scale wood composition is suspected to generate both signal classes within similar sizes (peak amplitude).

- Signals of class c1 dominate the AE activity, and thus the damage accumulation significantly. For the ultimate failure of plywood samples, c1 is rather less of relevance.
- A predictor by means of c2 might be found for some material designs (solid spruce wood and plywood 4) and load cases by the changing amplitude distribution of c2 signals detected at several load stages. The amplitude distribution considers peak amplitude and its relative frequency, which might give the prediction of significant crack size of the c2 signals whose source mechanisms are the most relevant for the ultimate tensile strength.
- Extrapolation from AE Felicity-ratio versus load level is an alternative approach to failure load and possibly also failure location prediction (see, e.g., Fowler et al. 1989), but that requires a specific stair-step load pattern.

6 REFERENCES

Baensch F, Sause MGR, Brunner AJ, Niemz P. 2015 *Damage Evolution in Wood – Pattern Recognition based on Acoustic Emission Frequency Spectra*. Holzforschung, 69(3), 357-365.

Brunner AJ, Nordstrom R, Flüeler P. 1995. *A Study of Acoustic Emission-Rate Behavior in Glass Fiber-Reinforced Plastics.* Journal of Acoustic Emission, 13(3-4), 67-77.

Brunner AJ, Nordstrom RA, Flüeler P. 1997. *Fracture phenomena characterization in FRP-composites by acoustic emission.* European Physical Society (EPS), 21B, 83-84.

Brunner AJ, Howald M, Niemz P. 2006. *Acoustic Emission Rate Behavior of Laminated Wood Specimens under Tensile Loading.* Progress in Acoustic Emission XIII, (Eds. M. Enoki, M. Takemoto, H. Cho), 367-372.

Brunner AJ. 2018. *Identification of damage mechanisms in fiber-reinforced polymer-matrix composites with Acoustic Emission and the challenge of assessing structural integrity and service-life.* Construction and Building Materials, 173, 629-637.

Chen Y, Ziehl P, Ramirez G, Fowler TJ. 2007. *Effect of Temperature on Acoustic Emission Evaluation of FRP Vessels (Tensile Specimens).* Transactions of the ASME, 129, 516-524.

DIN 52377. 2016. *Testing of plywood - Determination of modulus of elasticity in tension and of tensile strength.* DIN Deutsches Institut für Normung, 1-9.

Fowler TJ, Blessing JA, Conlisk PJ, Swanson TL. 1989. *The MONPAC System.* Journal of Acoustic Emission, 8(3), 1-8.

Gostautas RS. 2007. *Identification of failure prediction criteria using acoustic emission monitoring and analysis of GFRP bridge deck panels.* Report No. K-TRAN: KU-02-1, 1–85.

Ichikawa D, Kitamura M, Yuqiu Yang YQ, Hamada H. 2014. *Mechanical Properties of the Multilayer Laminated Intra-Hybrid Woven Fabric Composites.* Proceedings ASME 2014 International Mechanical Engineering Congress and Exposition, Volume 14, 1-7.

Jinen E. 1990. *The fracture energy and Acoustic Emission of a short carbon fiber reinforced Nylon-66 Composite.* Engineering Fracture Mechanics, 37(6) 1183-1194.

Lysak MV. 1996. *Development of the theory of Acoustic Emission by propagation cracks in terms of fracture mechanics*. Engineering Fracture Mechanics, 55(3), 443—452.

Ritschel F, Sause MGR, Brunner AJ, Niemz P. 2014. Acoustic Emission (AE) signal classification from tensile tests on plywood and layered wood. Proceedings EWGAE-Conference, German Society for Nondestructive Testing, BB 149-CD, 1-7.

Ritschel F, Zhou Y, Brunner AJ, Fillbrandt Th, Niemz P. (2014) *Acoustic emission analysis of industrial plywood materials exposed to destructive tensile loads.* Wood Science and Technology, 48(3), 611-631.

Sause MGR, Gribov A, Unwin AR, Horn S. 2012. *Pattern recognition approach to identify natural clusters of acoustic emission signals.* Pattern Recognition Letters 33, 17–23.

Vergeynst L, Sause MGR, Ritschel F, Brunner AJ, Niemz P, Steppe K. 2014. *Finite element modelling used to support wood failure identification based on acoustic emission signals.* Proceedings COST – Timber Bridge Conference, 141-146.

Warnet L, Akkerman R, Reed PE. 2003. *The effect of residual stress on transverse cracking in cross-ply carbon polyetherimide laminates under bending.* ESIS Publication 32, 465-476.